RSC Advances

Poly (caprolactone)-Poly (ethylene glycol) - Poly (caprolactone) (PCL-PEG-PCL) Nanoparticles: A Valuable and Efficient System for in vitro and in-vivo Delivery of Curcumin

Journal:	*RSC Advances*
Manuscript ID	RA-ART-11-2015-024942.R1
Article Type:	Paper
Date Submitted by the Author:	27-Dec-2015
Complete List of Authors:	danafar, hossein; school of pharmacy, kheiri, hamidreza; school of pharmacy sharafi, ali; school of pharmacy Ramazani, Ali; Zanjan University of Medical Sciences ghasemi, mohammad hossein; zanjan
Subject area & keyword:	Nanotechnology < Chemical biology & medicinal

Poly (caprolactone)-Poly (ethylene glycol) - Poly (caprolactone) (PCL-PEG-PCL) Nanoparticles: A Valuable and Efficient System for *in vitro* and *in-vivo* Delivery of Curcumin

Hamidreza Kheiri Manjili[1, 2], Ali Sharafi[3, 4, 5], Hossein Danafar[1, 6*], Mirjamal Hosseini[5], Ali Ramazani[4], Mohammad Hossein Ghasemi[3, 6]

[1]Pharmaceutical Nanotechnology Department, School of Pharmacy, Zanjan University of Medical Sciences, Zanjan, Iran

[2]Zanjan Pharmaceutical Nanotechnology Research Center, Zanjan University of Medical Sciences, Zanjan, Iran

[3]Zanjan Pharmaceutical Biotechnology Research Center, Zanjan University of Medical Sciences, Zanjan, Iran

[4]Cancer Gene Therapy Research Center, Zanjan University of Medical Sciences, Zanjan, Iran

[5]Applied Pharmacology Research Center, Zanjan University of Medical Sciences, Zanjan, Iran

[6]Department of Medicinal Chemistry, School of Pharmacy, Zanjan University of Medical Sciences, Zanjan, Iran

*Corresponding Author's E-mail: danafar@zums.ac.ir

Abstract:

Among the potent anticancer agents, curcumin is known as an effective agent against many different types of cancer cells. Its clinical applications have been limited because of hydrophobicity, low gastrointestinal absorption and fast metabolism. In the present study, curcumin was encapsulated within PCL-PEG–PCL micelles through a single-step nano-precipitation method, leading to creation of Cur/ PCL-PEG–PCL micelles. PCL-PEG–PCL copolymer was characterized *in vitro* by HNMR, FTIR, DSC and GPC techniques. PCL-PEG–PCL copolymers with curcumin were self-assembled into micelles in aqueous solution. The resulting micelles were characterized further by various techniques such as DLS and AFM. Anti-tumor properties of curcumin-loaded micelle evaluated in cancer cell lines in both *in vitro* and *in vivo*. The results showed the successful formation of spherical curcumin-loaded micelles. The encapsulation efficiency of curcumin was 83±1.29%. The results of AFM revealed that the

micelles have spherical shapes with size of 70.34 nm. *In vitro* release of curcumin from curcumin-entrapped micelles was followed remarkably sustained release profile. The curcumin-loaded micelle showed an efficient physical stability and high loading efficiency. The results of *in vivo* experiments indicated that the curcumin-loaded micelle significantly reduces the tumor size, prolongs the survival and increases the splenocyte proliferation and IFN-γ production as well as a significant decrease the IL-4 production. The results indicate the successful formulation of curcumin loaded PCL-PEG–PCL micelles and nanoformulation have a significant chemopreventive effect on cancer cell lines through cell proliferation inhibition, apoptosis induction and anti-tumor immunity stimulation.

Keywords: Curcumin, Drug delivery, Micelles, PCL-PEG–PCL

1. Introduction

The chemical formula of curcumin (CUR) is 1, 7-bis (4-hydroxy-3-methoxyphenyl)-1, 6-heptadiene-3, 5-dione with a chemical structure in the keto–enol tautomerism. Natural poly phenolic compound curcumin is a low molecular weight yellowish pigmentation of turmeric (*Curcuma longa* L.) which is widely used as a food flavor and coloring agent. It can isolate from the rhizome of turmeric. Curcumin is also an interesting therapeutic agent because of its remarkable biological properties including low toxicity, antioxidant, anti-inflammatory, anti-microbial, antitumor and wound healing activities[1-4]. Curcumin can use for the treatment of various diseases, especially cancer. It has the ability to inhibit carcinogenesis in a variety of cell lines[5-7]. The ability of curcumin to induce apoptosis in cancer cells without cytotoxic effects on healthy cells makes it a valuable candidate for drug delivery against cancer[8-10]. Nevertheless, its clinical potential has been greatly limited due to extremely low solubility in aqueous solution under acidic or neutral conditions, high decomposition rate in an alkaline media and photo degradation in organic solvents as well as its poor bioavailability[11-14]. For solving these limitations, many efforts to increase the solubility and stability of curcumin have been described, e.g. the use of curcumin nanoparticles[15], the inclusion of curcumin into central cavities of cyclodextrins[16], the use of curcumin- encapsulated microemulsions[17] and curcumin-loaded O-carboxymethyl chitosan nanoparticles or curcumin-loaded chitosan nanoparticles[18]. In recent years, many chemotherapeutic formulations have been developed. Copolymeric nanoparticles (NPs) have numerous advantages including their stability and simple surface modification[19]. Both controlled drug release and disease-specific localization could be achieved by tuning the polymer characteristics and surface chemistry. Hydrophobic biodegradable polymeric NPs can act as a local drug depot and providing a source for a continuous supply of encapsulated therapeutic compound(s) at the disease site (such as at solid tumors). To achieve drug controlled release, biodegradable polymeric nanoparticles are

often used in advanced anticancer drug delivery systems[20, 21].Some drug delivery systems *via* biodegradable polymer such as nanoparticles delivering anticancer agentsare commercially available[22]. Poly (caprolactone) -poly (ethylene glycol) - Poly (caprolactone) (PCL-PEG-PCL) copolymers are biodegradable, easy to produce, amphiphilic character and have a strong potential application in drug delivery systems[23-25]. In order to improve therapeutic efficiency of curcumin, various approaches for encapsulating of curcumin has been introduced recently such as: Liposomal curcumin[26], PEG-curcumin conjugate[27] and PCL-PEG-PCL nanofibers encapsulating curcumin[28, 29]. For this reason, it seems that encapsulating of curcuminin PCL-PEG-PCL micelles as a novel delivery vehicle for curcumin in *in vitro* and *in vivo* cancer therapy.

2. Materials and methods

2.1. Materials

Curcumin (Merck, Darmstadt, Germany, Art No. 820354), stannous 2-ethyl-hexanoate (Sn (Oct) 2) (Aldrich, St. Louis, USA, CAS. 301100), PEG (Mn=6000 Da) (Aldrich, St. Louis, USA, CAS.81323), ε-caprolactone (98% purity) (Aldrich, St. Louis, USA, CAS.502443) and other chemicals and solvent were purchased.

2.2 *Synthesis of PCL-PEG-PCL copolymer*

The synthesis of PCL-PEG–PCL copolymer by a ring opening polymerization of ε-caprolactone with PEG as initial molecule and Sn (Oct) $_2$ as catalyst was performed[29]. The polyethylene glycole was kept under a high vacuum at 80°C for 2 h to remove all moisture. Briefly, ε-caprolactone (4 g), PEG (2 g), and Sn (Oct) $_2$ (0.01 mmol) were heated to 120°C under a nitrogen atmosphere. The polymerization reaction was performed with stirring situations. After 12 h, the resulting product was cooled to room temperature (23°C), dissolved in dichloromethane, and precipitated in cold diethyl ether. Then the mixture was

filtered and the purification process was repeated twice more. The obtained tri block copolymer was dried under vacuum at room temperature for 24 h.

2.3. Characterization of tri block copolymer

Proton Nuclear Magnetic Resonance Spectroscopy (1H NMR) in CDCl3 at 400 MHz (Bruker, Evans, 400) and Fourier Transform Infrared spectroscopy (FT-IR) (Bruker, Tensor 27) were used for characterization of the chemical structure of the PCL-PEG-PCL copolymer. Molecular weight and distribution of the PCL-PEG-PCL copolymers were calculated by gel permeation chromatography (GPC) (Knaure, Berlin, Germany) composed of with an ultra styragel column and differential refractometric detector (4.6×30 mm) (Waters, Milford, USA, model HR 4E). Tetrahydrofuran (THF) as a mobile phase was with a flow-rate of 1 ml/min and the injection volume was 100 µl of stock solutions (0.1-0.5 w/v %). The standards of polystyrene monodisperse in the range of 4500- 29500 DA (Varian Palo Alto, CA) obtained before measurements for use as the calibration curve for determination of average molecular weight of the PCL-PEG-PCL copolymers. Thermal analysis of tri block copolymers was determined by differential scanning calorimetry (DSC) (Mettler Toledo, model Star SW 9.30). Copolymers were heated at a rate of 10 °C min^{-1} and the data were recorded from 0 to 250 °C.

2.4. Preparation of micelles

Nano precipitation method for used to loading of curcumin to the nanoparticles and chloroform as the solvent[30]. PCL-PEG-PCL copolymer (20 mg) and curcumin (6 mg) were dissolved in 2 ml of chloroform. The solution was added drop-wise through a syringe (G=22) into 25 ml of distill water under certain mixing rates and was continuously stirred magnetically at room temperature for evaporation of the organic solvent. After removing of chloroform by rotary vacuum evaporation at 35°C, the resulting yellowish aqueous solution

was filtered through a 0.45 μm filter membrane to remove the unloaded CUR. Curcumin loaded micelles were obtained by self-associate of amphiphilic PCL-PEG-PCL copolymers. The resulting molecules by centrifuging at 20000 g for 20 min were separated and freeze-dried under a pressure of 14 Pa at -78 °C until two separate all the residual solvents and to obtain the final dried form.

2.5. Characterization and physicochemical properties of the nanoparticles

2.5.1. Particle morphology

Atomic Force Microscopy (AFM) (JPK, Berlin, Germany, model Nano Wizard 2) was used to observe of morphology. One drop of micelles sample was diluted in water and a droplet of 2 μL was placed on a freshly cleaved mica substrate (1 cm^2) followed by air-drying. Measurements of AFM were performed in intermittent contact mode.

2.5.2. Particle size and zeta potential curcumin loaded micelles

Dynamic Light Scattering (DLS) using a nano/zetasizer (Malvern Instruments, Worcestershire, UK, model Nano ZS) was used for determination of the particle size distribution zeta potential of the prepared micelles.

2.5.3. Stability of micelles

For evaluation of physical stability of micelles, the particle size distribution of the micelles was monitored by suspension of micelles in phosphate-buffer saline (PBS, pH=7. 4) and kept at ambient temperature at times 0, 15, and 30 days after preparation using the method described in 2.4.

2.5.4. Drug loading and encapsulation efficiency

Two parameters drug loading ratio and encapsulation efficiency of micelles for determination of drug loading and encapsulation efficiency of curcumin in the micelles were evaluated.

The drug loading ratio was evaluated by equation 1[31].

$$\%\mathrm{DL} = \frac{\text{weight of drug in micelles}}{\text{weight of micelles}} \times 100 \quad (1)$$

$W_{\text{drug in micelles}}$ and W_{micelles} show weight of the encapsulated drug and the total weight of the corresponding drug-encapsulated micelles, respectively. DL% is the drug loading ratio (%).

For evaluation of the drug loading ratio, 1 mg of the final freeze-dried nano dispersion was dissolved in 1 ml of dichloromethane. The drug entrapment was determinate by high performance liquid chromatography (HPLC). The mobile phase consisted of methanol and 5% (w/v) acetic acid in the volume ratio of 70:30, and was delivered at a flow rate of 1.0 ml/min using a double-reciprocating pump and the analysis wavelength was at 420 nm (Waters, MA, USA, model Breeze).. The sample was injected through a 50 µL sample loop. AC18 analytical column (4.6 mm, particle size 5 µm; Perfectsill, MZ-Analysen, 250 mm Technik, Germany) equipped with a guard column of the same packing was used. Encapsulation efficiency obtained using the following equation 2:

$$\mathrm{EE}\% = \frac{(\text{weight drug in micelles})}{\text{weight of initial drug}} \times 100 \quad (2)$$

2.5.5. FTIR analysis

It is possible to obtain some information about the occurrence of possible interaction(s) between substances involved in a nanocarrier system using FTIR analysis. Mostly, the interaction between drug and polymer is investigated through the band shifts by the functional groups as well as through broadening in IR spectra compared to their individual spectra. To confirm the presence of any interactions between drug and polymer, the FTIR

spectra of solid micelles were compared with pure drug and individual polymers. Freeze-dried samples were pressed to form the standard disks and the FTIR spectra of the KBr disks were recorded using the abovementioned instrument from 600 to 4000 cm^{-1}.

2.5.6 DSC analysis

Any possible drug-polymer interaction(s) as well as the physical changes occurred on the drug or polymer can be studied using the thermal analysis. DSC analysis was carried out on pure drug and drug-loaded micelles. Samples were heated at a rate of 10 ° C min^{-1} and the data were documented from 0 to 200 °C.

2.6. Drug release study to in vitro

Profile release of curcumin from micelles to *in vitro* was determined by the direct dispersion method as described in the literature[18, 32, 33].This test was performed to measure the release behavior of curcumin from nanoparticles. At first, 5 mg of freeze-dried drug-loaded curcumin were dispersed in 2 ml phosphate-buffered saline (PBS) with pH= 7.4 and the resulting suspension was placed within a dialysis sac (MW 12 kDa) and incubated at 37 °C while immersed in 15 ml of PBS. Then, at predetermined time intervals, 3 ml of the dialysate was taken out and replaced by 3 ml fresh PBS. The concentration of curcumin in the dialysate was determined by HPLC analysis, at 420 nm wavelength. All the release studies were performed in triplicate. As the release control, the release of void curcumin was measured in PBS at pH= 7.4.

2.7. Cell culture

Experiments were carried out on mouse breast adenocarcinoma (4T1), human breast adenocarcinoma (MCF7), human prostate cancer (PC-3) cell lines and human mammary epithelial (MCF10A), were purchased from the Pasteur Institute (Tehran, Iran). The cells

were cultured in RPMI-1640 (GIBCO, USA) for 4T1 cells and standard DMEM- medium (GIBCO, USA) with 10% heat-inactivated FBS (GIBCO Laboratories, Cergy-Pontoise, France), 500 µg/ml geneticin (G418), 300 µg/ml glutamine, 0.25 µg/ml fungizone, 100 µg/ml streptomycin, and 100 units/ml penicillin for MCF7 and PC-3 and DMEM/F12 1:1 (Life Technologies, Hyclone, Cellgro) that supported by horse serum %0.25, hydrocortisone (1 mg/ml), cholera toxin (1 mg/ml), insulin (10 mg/ml) and Pen/Strep for MCF10A cell line .The cell lines were adherent and grew as mono layers at 37°C in a humidified atmosphere 5% CO_2 incubator. The cells were harvested with 0.5 g/l trypsin (GIBCO Laboratories) and 0.2 g/l EDTA (GIBCO Laboratories) after 80% confluency for 3 minutes in 37°C. The concentration of the cells in the culture was adjusted to allow for exponential growth.

2.8. Cytotoxicity of PCL-PEG-PCL Micelle

For performing the MTT (3-[4, 5-dimethylthiazol-2-yl] 2, 5-iphenyltetrazolium bromide) assay, 96 well plates were utilized[34]. Cells were seeded onto plates and permitted to adhere and grow overnight in 200 µl medium with 2×10^3 cells per well concentration. The cells (cancer cells and normal cells as control) were then incubated with fresh medium, including serial concentrations (0 to 100 µM) of curcumin-loaded nanoparticle (cur / PCL-PEG–PCL) for 12 h, 24 h, 48 h and 72 h. One group without treatment was considered as a control. The MTT solution at appropriate concentrations (10 µl of 5 mg/ml MTT solution in each 100 µl media) was added to each well and the plates were incubated at 37°C in a humidified atmosphere containing 95% air and 5% CO_2 for 4 hours. Following the incubation, the remaining MTT solution was removed and 100 µl of DMSO was added to each well to dissolve the formazan crystals. The plates were shaken for 10 minutes on a plate shaker to ensure adequate solubility. The amount of formazan was determined by measuring the absorbance at 570 nm using an ELISA plate reader (with a reference wavelength of 690 nm). The control wells for absorbance readings contained no cells or medium, but similarly the

DMSO was added to them. All experiments were arranged in triplicates and repeated twice for statistical analysis. Results were expressed as Mean ± SD[35].

2.9. Total RNA extraction and Real-Time PCR

Total RNA was extracted from the nanoformalision -treated or control cell line with TRIzol (GIBCO), according to the manufacturer's instructions. Quantity of RNA concentrations were quantified by measuring OD260/280. The A260/A280 ratio of extracting RNA was about 1.75-1.95 using a Nanodrop-2000c spectrophotometer (Thermo scientific, USA).Complementary DNAs was synthesized with oligo-dT primers in a 25µl total volume reaction mixture using a superscript pre-amplification system (Invitrogen, USA). We used Primer Express software to design primers for endogenous and target genes. We used glyceraldehyde-3-phosphate dehydrogenase (GAPDH) gene as the reference gene with forward primer:5'-ACTAACCCTGCGCTCCTG-3' and reverse: 5'-CCCAATACGACCAAATCAGA-3', and C-myc with forward primer:5'-CTACCCTCTCAACGACAGCA-3'and reverse primer:5'-GAGCAGAGAATCCGAGGAC-3';Bcl-2 with forward primer: 5'-CTTTACGTGGCCTGTTTCAA-3' and reverse primer:5'-CTGAAGGACAGCCATGAGAA-3'; BAX with forward primer:5'-AGCTGCAGAGGATGATTGC-3' and reverse primer:5'-GTTGAAGTTGCCGTCAGAAA-3'; Bcl-xl, whit forward:5'-AAGGAGATGCAGGTATTGGTGAGT-3', reverse primer:5'-CCAAGGCTCTAGGTGGTCATTC-3'. The expression levels of genes were calculated with Real-Time PCR using ABI prism 7500 sequence detection system (Applied Bio systems, USA). Amplification reactions contained 5µL of cDNA, 10 µL of Sybr Green-I dye (Applied Bio systems) and 0.3 µL of each of the specific primers. The concentration of primers in the final volume of 20 µL was 100 nM. PCR performed with initiating one cycle at 95 °C for

10 min, then 40 cycles at 95°C for 15s and at 59°C for 45s. The real-time PCR was evaluated by the melting curve analysis.

2.10. Apoptosis Assay for the In Vitro Study

The flow cytometry experiment was used to determine the percentage of apoptosis and necrosis cells which subjected to IC_{50} concentrations of nanoformulation, at 12, 24, 48, hours after treatment using Annexin V–FITC and propidium iodide (PI) stain on MCF-7 and 4T1 cell lines. Phosphatidyl serine flipping from the internal to the external layer of plasma membrane is one of the main earliest apoptotic aspects. After harvest the cell lines with trypsin, the cells were counted and then dispensed into 6-well culture plates with approximately 10000 cells/well. Apoptosis was evaluated using the Annexin V-FITC Apoptosis Detection Kit (Biovision, Inc). Briefly, cells were trypsinized and centrifuged at 400g for 5 min, then resuspended the plate with 500 μL of 1X binding buffer and then treated with 5 μL of Annexin V–FITC and 5 μL PI and transferred to FACS tubes for analysis in a flow cytometer (BD Bioscience FACS, USA) after mixing and incubation for 8 min at room temperature. Samples were evaluated by flow cytometry [36]. Cells in media alone, lacking of nanoparticles (as the negative control) and cells treated with bare nanoparticle were also analyzed in the same approach. Flow cytometry experiments were replicated three times and the average of the results was calculated.

2.11 Animals

2.11.1 Tumor models

6–8 weeks age of female inbred BALB/c mice were purchased from the Pasteur Institute, Tehran, Iran, and kept under the standard conditions. Animal care and treatment was performed in coincidence with the guideline of Animal Care and Research Committee of the

Zanjan university of medical sciences, which is in conformity with the Guide for the Care and Use of Laboratory Animals[37]. A total of 1×10^6 4T1 cells/ 200 µl of PBS in logarithmic growth phase were injected subcutaneously (s.c.) into the right flank of BALB/c mice. Once tumor mass became established on 8thday because of aggressive and rapid growth properties of 4T1 cell line, animals were randomized into 4 groups (n=6 per group) including two test groups receiving intraperitoneally 12.5 mg/kg bw (body weight) of curcumin loaded nanoparticle and void curcumin for three weeks as well as two control groups obtaining copolymers and PBS (as negative control). Tumor volume (mm^3) was measured three times per week using a digital vernier caliper (Mitutoyo) until sacrificing mice on day 38 post injection. On the other hand, the changes in median survival time (% IST) were also calculated for all 4 treatment groups. The institutional review board (IRB) of the Zanjan University of Medical Sciences approved the procedure of survival study in tumor-bearing mice. The tumor volume (mm^3) and median survival time (% IST) were calculated by Eqs. (1) and Eqs. (2) Respectively[38].

Esq. (1): Tumor volume = ½ [Tumor length× (Tumor width) ^{2}]

Esq. (2): IST= [T/C]

(T is median survival time of treated group and C is control group)

2.11.2 Splenocytes proliferation index

While the mice (n=6 per group) were sacrificed, splenocytes proliferation index was followed by spleen isolation [The effect of vaccination with the lysate of heat shocked tumor cells on nitric oxide production in BALB/c mice with fibrosarcoma tumor] Spleen tissues were washed twice with PBS, homogenized and passed through a 100 µm filter to obtain a single cell suspension. Density gradient centrifugation over Ficoll/Hypaque were exercised for separation of viable

splenocytes and viable cells were determined by trypan blue (Sigma-Aldrich, USA) exclusion[39]. Tumor lysate, PHA (GIBCO) as positive control and medium as negative control with 1×10^5 concentration of splenocytes/well in a total volume of 200 µl of completeRPMI-1640 medium was cultured and incubated for 5 days at37 °C in 5% CO_2 humidified atmosphere. MTT assay was performed for determining of the splenocytes proliferation index. Each experiment was accomplished in triplicate wells.

2.11.3 Body Weight Measurements

Changes of body weight were measured in one day before administration, initiation of administration, 1, 5, 10, 15, 20, 25, 30, 35 and 40 days after initiation of administration with sacrifice using an automatic electronic balance, respectively. At start of administration and at a termination, all animals were fasted overnight (lacking water for 12 hrs.) to reduce the differences from feeding.

2.11.4 Enzyme-linked immunosorbant assay (ELISA) for measuring Cytokines

To evaluate whether the cytokine release is influenced by tumor lysate, we incubated the splenocytes with tumor lysate, PHA as positive control and medium as negative control in a density of 1×10^6 cells/well on 24-well plates [The effect of vaccination with the lysate of heat shocked tumor cells on nitric oxide production in BALB/c mice with fibrosarcoma tumor]. Then, supernatant was collected and tested for IFN-γ and IL-4 by commercially available sandwich based ELISA kit (R&D, Minneapolis, USA) according to the manufacturer's instruction. Statistical analysis all data are expressed as the Mean ± SD of at least three experiments[40].

2.12. Statistical analysis

All experiments were performed in triplicate and analyzed by one-way analysis ANOVA (Graph pad Prism) for significant differences. P values of <0.05 were considered statistically significant. Data are presented as a mean value ± SD (n = 3 measurements).

3. Results

3.1 Synthesis and characterization of PCL-PEG–PCL copolymer

Triblock copolymers were successfully synthesized using the ring-opening polymerization of caprolactone in presence of PEG, whose hydroxyl end group initiated the ring opening. Characterization of the PCL-PEG–PCL tri-block copolymer structure was evaluated by HNMR spectroscopy in CDCl3 (Fig 1). The presence of ethylene's (CH_2) in PCL was observed around 1.3 ppm, 1.6 ppm, 2.2 ppm and 4.06 ppm, the methylene (CH_2) groups of PEG were around 3.64 ppm. Table 1 shows the characteristics of synthesized copolymer[41]. FT-IR spectrum of PCL-PEG–PCL copolymer was shown in Fig 5b.The sharp and intense bands at 1725cm^{-1} and 1109cm^{-1}were attributed to the presence of carboxylic ester (C=O) and ether (C–O) groups, The signals at 2995and 2891cm-1 were assigned to the absorption of the C-H stretching bonds of -CH_2CH_2, which are similar to those of ε-CL. The PCL-PEG–PCL copolymer formation carried out successfully [42].Fig 2 shows the GPC spectrum of PCL-PEG-PCL. The single peak indicating the mono-distribution of macromolecular weight and absence of any homopolymer ε-CL or PEG; and shows that no Tran's esterification or backbiting reactions occurred during polymerization [43]. The results designated that the weight- and number-based average molecular weights of copolymer were 20.4 and 17.5 KDa, respectively.

3.2 Preparation and characterization of copolymeric micelles

AFM was used for confirmation of nanoparticles. As expected for the micelles, the PCL-PEG–PCL copolymeric micelles showed a homogeneous spherical morphology (Fig. 3).The size of copolymric micelle measured by AFM was about 70.34 nm. The size of micelles measured by AFM to compare with measuring by DLS was smaller because the size measured by AFM is related to the collapsed micelles after water evaporation while micelle diameter measured by DLS represents their hydrodynamics diameter[44]. The size of nanoparticles was also measured by dynamic light scattering technique (Fig 4).The Z-average and Zeta potential of curcumin loaded PCL-PEG–PCL micelles were determinate about 99.07 nm and -5.58 mv, with their corresponding PDI being 0.181. The encapsulation efficiencies and loading ratio of curcumin loaded to copolymeric micelles were determined 83 ± 1.29%, and 17% ± 1.23% respectively.

3.3. FT-IR analysis

Fig. 5 illustrates the FTIR spectra of PCL-PEG-PCL copolymer, curcumin, and curcumin-loaded PCL-PEG-PCL micelles. The FTIR spectrum of curcumin shows characteristic bands appeared at 3515.77 cm^{-1} (O-H, stretching) for phenolic hydroxyl group, 1630.97 cm^{-1} (C=C, stretching), 1512.94 cm−1 (C=C band of benzene), and 856.38 cm^{-1}(C-H, stretching of aromatic ring) (Fig.5). Comparing these data with the drug-loaded micelles spectrum exhibits the presence of curcumin characteristic peaks in the spectrum of micelles which could demonstrate the successful loading of curcumin in the nanoparticles. The most striking feature of the FT-IR spectra of micelles was the blue shift of the C=O vibration, from 1725.25 to 1730.56 cm^{-1} for drug-loaded PCL-PEG-PCL micelles compared to the copolymer spectrum. The shift in the micelles spectrum indicates that there exist some form(s) of association between curcumin and C=O functional group of copolymer[31]. All results

indicated that Cur may be present in a dispersed condition in the nanoparticulate Cur formulation[45].

3.4. DSC analysis

Fig. 6 shows the DSC thermograms corresponding to PCL-PEG-PCL copolymer, curcumin and micelles loaded by curcumin. The thermogram of PCL-PEG-PCL copolymer displayed an endothermic peak at 58.68 $^{\circ}$C which is indicative for the melting of the crystalline PCL segment of copolymer, the thermogram of curcumin displayed an endothermic peak at 176.71 $^{\circ}$C and micelles displayed two endothermic peaks at 49.09 ^{0}C and 175.55 ^{0}C which stand for the melting of copolymer and curcumin association in the form of micelles. This endothermic peak of micelles presumably confirms a physical interaction between copolymer and curcumin upon loading of the drug in micelles, since the melting point of PCL micelles was lower than melting point of both copolymer (58.68 $^{\circ}$C) and purecurcumin (176.71 ^{0}C).

3.5.1. Curcumin release from micelles impacted by different release media

Study of curcumin release in order to test the impact of the biochemical and chemical factors on the release of curcumin from micelles was determined on curcumin-loaded copolymeric nanoparticles in neutral and acidified PBS solution (pH=5.5).The release of void curcumin was evaluated to verify that the diffusion of drug molecules across the dialysis membrane was not a rate-limiting step during the release process[46]. The release of void curcumin was rapidly released and reached to75.95% of the total amount in 12 hours. The release profiles of curcumin from the curcumin-loaded micelles, at pH 7.4, 5.5, and plasma illustrate at Fig. 7. No importance initial burst curcumin release showed from the micelles. As it can see Fig. 7, with pH decreasing from 7.4 to 5.5, the curcumin release from nanoparticles was increased. For example, percentage of curcumin released from the micelles after 96 h incubation, in the media with pH values of 7.4, 5.5 and human plasma were about 60.99, 65.56, and 63.54%,

respectively, Fig. 7 shows that the maximum curcumin releases form micelles is 72.01%, 76.67% and 74.69% for PBS pH=7.4, pH=5.5 and plasma after a period of 120 h respectively. The reason of curcumin sustained release can be related to the encapsulated of curcumin in inner part of micelles or the core of micelles. Therefore, copolymeric micelles can be stay on as highly sensitive and selective nano-systems for controlled drug delivery for hydrophobic drugs to access of different therapeutic objectives.

3.6. Physical stability of micelles

Evaluation size stability of nanoparticles is very important to the clinical administration of nanoparticle dispersions, because the characterized both of the particle structure integrity and as an indicator of the possible inter-particular aggregation. For this reason, in these studies, the size stables of the particle were determinate over a 30-days course. Table 2shows the variation of the sizes of micelles as a function of incubation time. Slightly increasing was seen to the size of all micelles throughout the measurement period. This observation cannot be a sign of aggregation, which usually leads to several fold increases.

3. 7. Cell viability

The *in-vitro* investigation of the toxicity of Cur@ [PCL-PEG-PCL] NPs on MCF-7, 4T1and PC3 cancerous cell lines as well as MCF10A cell line were performed using MTT assay (Fig. 8). Cur@ [PCL-PEG-PCL] NPs considerably repressed the proliferation of MCF-7, 4T1 and PC3 cancerous cell lines in a time-dependent manner in compare with the human mammary epithelial cell line ($P < 0.01$). The IC_{50} value of Cur@ [PCL-PEG-PCL] NPs for MCF-7 cell lines within 12, 24, and 48 h were 32, 22 and 14 μM, respectively which increased to 15 μM in 72 h. The IC_{50} values of Cur@ [PCL-PEG-PCL] NPs for 4T1 cells were 37, 33 and 24 μM for 12, 24 and 48 h, respectively which decreased to13 μM after 72 h. Also, the IC_{50} values of Cur@ [PCL-PEG-PCL] NPs for PC3 cells were 42, 38 and 21 μM for 12, 24 and 48 h,

respectively which reached to10 μM for 72 h. In contrast, the same concentrations of Cur@ [PCL-PEG-PCL] NPs did not affect the proliferation of MCF10a cells which can verify the safety and biocompatibility of Cur@ [PCL-PEG-PCL] NPs on the human mammary epithelial cell line. The experiments were separately done in triplicate for four cell lines.

3. 8. Detection of cell apoptosis by Flow Cytometry

To determine the toxicity effects thorough the apoptosis for Cur@ [PCL-PEG-PCL] NPs, MCF-7 and 4T1 cell lines were incubated with IC_{50} concentrations of Cur@ [PCL-PEG-PCL] NPs for 12, 24 and 48 h(Fig. 9).The statistical analysis of flow cytometry results with two-way ANOVA and Bonferroni post-test demonstrated that the percentage of live cells (A-/PI-) decreased significantly ($P<0.0001$) after treatment with Cur@ [PCL-PEG-PCL] NPs in comparison with untreated cells (control group). It also decreased significantly ($P<0.0001$) in a time - dependent manner for MCF-7 and 4T1 cell lines. The percentage of early (A+/PI-) and late (A+/PI+) apoptosis increased significantly in the case of Cur@ [PCL-PEG-PCL] NPs, in compared with untreated cells (control group). Percentage of total apoptosis (early apoptosis + late apoptosis) considerably increased ($P<0.0001$) by 20.37-97.4% and 21.3-94.8% in a time-dependent manner for MCF-7 and 4T1 cell lines respectively.

3. 9. Gene expression profile

To study the effects of void Cur PCL-PEG-PCL micelles and Cur@ [PCL-PEG-PCL] NPs on human breast cancer cell lines (MCF-7), the mRNA expression of selected genes were analyzed by real-time PCR. The expression of BCL-2 gene was evaluated in a human breast cancer cell line treated or untreated with void Cur and Cur@ [PCL-PEG-PCL] NPs. Statistical analysis of real-time PCR results illustrate that after 72 h of 20 μM concentration treatment, the Cur@[PCL-PEG-PCL]NPs and void Cur significantly decreased the expression of BCL-2, 0.31 and 0.58 fold ($P<0.05$) of control group respectively. The

expression of BCL-xl gene in treated or untreated with void Cur and Cur@ [PCL-PEG-PCL] NPs. Cur@ [PCL-PEG-PCL] NPs significantly (P<0. 05) decreased levels of BCL-xlm RNA in comparison to void Cur and after 72 h the Cur@[PCL-PEG-PCL]NPs and void Cur decreased the expression of BCL-xl by 0. 39 and 0.75 fold (P<0.01) of control group, respectively. There was no significant difference observe in the BCL-xl gene expression with 20 μM of PCL-PEG-PCL micelles for72 h in compared to the untreated cells. The expression of BAX was increased significantly in response to treatment with Cur@ [PCL-PEG-PCL] NPs by 1.95 fold in compared to the untreated cells. In the case of void Cur expression of BAX was increased significantly by 1.37 fold in compare with untreated cells after 72 h (Fig. 10). In the Cur @ [PCL-PEG-PCL] NPs treated cells with 20 μM, at 72 h incubation, the expression of c-myc was significantly decreased 0.41 folds in compare to the untreated cells. Decreasing expression of c-myc by Cur@ [PCL-PEG-PCL] NPs, suggesting that Cur@ [PCL-PEG-PCL] NPs induces anti-metastatic effect in breast cancer cell lines (Fig. 10).

3. 10. Effect of curcumin nanoformulation (PCL-PEG-PCL) on tumor development and survival rate

The changes of tumor volume in four groups of mice were evaluated as shown in Figure (11 a). Data indicated that in day 20, the tumor growth was significantly (P<0.01) suppressed in mice treated with PCL-PEG-PCL nanoformulation in comparison with other groups which received void curcumin, copolymer and PBS. Meanwhile, as Figure (11 b) shows, mice treated with Cur@ PCL-PEG-PCL nanoformulation were still alive in day 80 compared to curcumin, PCL-PEG-PCL and PBS groups that succumbed by day 56, 53 and 44, respectively (P<0.05). Similar results were observed in two separate experiments.

Significant (P < 0.05) decreases of the body weights were demonstrated in all tumor-bearing mice as compared with intact control from 10 days after initial administration. curcumin loaded nanoparticle 12.5 mg/kg, 5-day intervals, intraperitoneally treated mice

showed significant decreases of body weights as compared with tumor-bearing control mice from 30 days after initial administration (Figure 12). However, void curcumin 12.5 mg/kg did not induce any meaningful body weight changes.

3. 11. Measurement of the lymphocyte proliferation index following treatment

All four groups of mice were tested for splenocytes proliferation index following tumor lysate, PHA (positive control) and medium (negative control) induction. The results showed significantly higher rates of splenocytes proliferation in the mice that receiving Cur@-PCL-PEG-PCL than those of three other groups ($P<0.05$) (Figure 13c). In the other hand the splenocytes did not show any significant differences in proliferation among groups when induced by PHA or medium (Figure13a and b).

3. 12. Measurement of IFN-γ and IL-4 level following treatment

As the results in Figure 14 indicate, splenocytes obtained from mice treated with Cur@-PCL-PEG-PCL, which were re-stimulated with tumor lysate, exhibited a significant ($P<0.05$) increase in the level of IFN-γ compared to those of other groups, though the overall level was slightly low in all samples. In addition, a significant decrease ($P<0.05$) was noticed in IL-4 production in mice receiving Cur@-PCL-PEG-PCL nanoformulation in comparison with other mice which were given void curcumin, PCL-PEG-PCL micelles and PBS. Data for samples stimulated with PHA (positive control) and medium (negative control) did not show any significant differences among groups (data not shown).

4. Discussion

Curcumin, a biologically active component of turmeric, has been used as an herbal medicine for the treatment of inflammatory disorders, cancer, acquired immune deficiency syndrome,

and other diseases for a long time[47, 48]. It has been found that it has preventive and therapeutic effects in various cancers, and has been confirmed to be a potent chemosensitizer[49]. The problem with using curcumin is that it is poorly soluble in water and is easily degraded by the body. Thus, curcumin cannot be used *via* the intravenous route, where it could possibly use a maximal pharmacological effect. PCL-PEG-PCL was employed in this study to prepare micelles, as described. To overcome the poor water-solubility of curcumin, curcumin was encapsulated into PCL-PEG-PCL micelles by a self-assembly method, producing curcumin /PCL-PEG-PCL micelles. Amphiphilic nature of PCL-PEG-PCL with hydrophilic PEG and hydrophobic PCL blocks provides an opportunity to form micelles in water. This behavior can be explained as a consequence of copolymer self-assembly into micellar structure because of its amphiphilic nature which, subsequently forces the hydrophilic PEG segments to serve as hydrophilic shell and the hydrophobic PCL segments to become the micellar core. The sizes of curcumin /PCL-PEG-PCL micelles by DLS were about 99.07 nm in diameter. Also, curcumin /PCL-PEG-PCL micelles showed drug loading of 17% ± 1.23% and a high encapsulation efficiency of 83± 1.29%, making it as an aqueous formulation of curcumin. In addition, the curcumin /PCL-PEG-PCL micelles had a negative surface charge of -5.58 mV, which increased the circulation time of the drug. Surface charge is important in determining whether the nanoparticles will cluster in blood flow or will adhere to or interact with oppositely charged cell membrane [50]. The plasma and blood cells always had a negative charge; nanoparticles with slight negative surface charge may minimize nonspecific interaction with these components through electrostatic interactions[51, 52]. The curcumin /PCL-PEG-PCL micelles were able to slowly release curcumin (Figure 7). The sustained release of curcumin from PCL-PEG-PCL micelles might be due to the diffusion of curcumin from micelles and the degradation or hydrolysis of micelles. In this work, we used PCL-PEG-PCL micelles to encapsulate curcumin. In the preparation process, curcumin and PCL-PEG-PCL

diblock copolymer mixture was first dissolved in chloroform solution, followed by evaporating the organic solvent. Then, the amphiphilic PCL-PEG-PCL copolymers self-assembled into supramolecular arrangements possessing a hydrophobic inner core and a hydrophilic shell in water, and curcumin self-assembled into the hydrophobic core of the micelles because of its hydrophobicity. The preparation procedure was simple and easy to scale up. These PCL-PEG-PCL micelles are biodegradable, biocompatible, amphiphilic, stable in blood, nontoxic, non-immunogenic, non-inflammatory, and small in size; these make PCL-PEG-PCL micelles an excellent candidate for drug-delivery systems[53]. Recent study showed that Cur@ [PCL-PEG-PCL] NPs is significantly nontoxic at doses required as a safe drug and could produce significant anti-cancer effects. *In vivo* studies on BCl-Xl gene expression, measurement of IFN-γ and IL-4 level showed the effects of the Cur@ [PCL-PEG-PCL] NPs and void Cur on expression of genes related to inflammatory and oxidative stress markers. T-test analysis demonstrated the expression of BCl-Xl gene was significantly decreased following treatment of Cur@ [PCL-PEG-PCL] NPs and void CUR in comparison with control groups. Also, significant rise in IFN-γ and decreased in IL-4 level was observed in treated animals when compared with control mice ($P<0.001$). In addition, down-regulation of BCl-Xl gene has a negative effect on the oxidative challenge and energy hemostasis change. Results of this study are in line with emerging studies suggesting the anti-oxidant and ROS scavenger effect of Cur@ [PCL-PEG-PCL] NPs and void Cur. Also, these results highlight the importance and safety of our suggestion NPs on energy hemostasis and anti-inflammatory responses *via* interactions of mitochondria and innate immune system. We propose that under oxidative stress conditions, impaired energy hemostasis and mitochondrial function result in ROS/RNS production that trigger immune-inflammatory responses by over-expression of BCL-Xl and increasing of IL-4. So, PCL-PEG-PCL micelle-encapsulated curcumin might be an interesting formulation to improve drug efficacy. In summary the

curcumin /PCL-PEG-PCL micelles improved the water solubility of curcumin and may have potential application in cancer treatment.

5. Conclusion

Methoxypoly (ethylene glycol)-poly caprolactone- (PCL-PEG-PCL) copolymer was synthesized and characterized by HNMR, FTIR, DSC and GPC techniques. Then, the PCL-PEG-PCL copolymer was self-assembled into micelles in aqueous solution in presence of curcumin. The resulting micelles were characterized by various techniques such as DLS and AFM. The encapsulation efficiency of curcumin was 83 ± 1.29%.The results of AFM revealed that the micelles formed had spherical structure with size of 70.34 nm. *In vitro* release of curcumin from curcumin-entrapped micelles was clearly sustained in all the media tested for this purpose, with the apparent release plateau reached late at about 130 h. Since Our NPs is non-toxic and can be categorized in wide therapeutic index drugs, it suggested one of the most popular in cancer treatment due to ability in decreasing of size, significant rise in IFN-γ and decreased in IL-4 level. Results showed that these NPs could be a good alternative approach in cancer treatment.

Acknowledgment

This work has been supported financially by Faculty of Pharmacy, Zanjan University of Medical Sciences, Zanjan, Iran.

References

1. Y. M. Sun, H. Y. Zhang, D. Z. Chen and C. B. Liu, *Organic letters*, 2002, **4**, 2909-2911.
2. S. Han and Y. Yang, *Dyes and pigments*, 2005, **64**, 157-161.
3. K. Kohli, J. Ali, M. Ansari and Z. Raheman, *Indian Journal of Pharmacology*, 2005, **37**, 141.
4. M. Panchatcharam, S. Miriyala, V. S. Gayathri and L. Suguna, *Molecular and cellular biochemistry*, 2006, **290**, 87-96.
5. A. Sun, M. Shoji, Y. J. Lu, D. C. Liotta and J. P. Snyder, *Journal of medicinal chemistry*, 2006, **49**, 3153-3158.

6. S. Somasundaram, N. A. Edmund, D. T. Moore, G. W. Small, Y. Y. Shi and R. Z. Orlowski, *Cancer research*, 2002, **62**, 3868-3875.
7. H. J. Kang, S. H. Lee, J. E. Price and L. S. Kim, *The breast journal*, 2009, **15**, 223-229.
8. B. B. Aggarwal, A. Kumar and A. C. Bharti, *Anticancer res*, 2003, **23**, 363-398.
9. H. Hatcher, R. Planalp, J. Cho, F. Torti and S. Torti, *Cellular and Molecular Life Sciences*, 2008, **65**, 1631-1652.
10. L. Ma'mani, S. Nikzad, H. Kheiri-Manjili, S. al-Musawi, M. Saeedi, S. Askarlou, A. Foroumadi and A. Shafiee, *European journal of medicinal chemistry*, 2014, **83**, 646-654.
11. H. H. Tønnesen, M. Másson and T. Loftsson, *International Journal of Pharmaceutics*, 2002, **244**, 127-135.
12. H. H. Tønnesen, J. Karlsen and G. B. van Henegouwen, *Zeitschrift für Lebensmittel-Untersuchung und Forschung*, 1986, **183**, 116-122.
13. K. Letchford, R. Liggins and H. Burt, *Journal of pharmaceutical sciences*, 2008, **97**, 1179-1190.
14. P. Anand, A. B. Kunnumakkara, R. A. Newman and B. B. Aggarwal, *Molecular pharmaceutics*, 2007, **4**, 807-818.
15. F.-L. Yen, T.-H. Wu, C.-W. Tzeng, L.-T. Lin and C.-C. Lin, *Journal of agricultural and food chemistry*, 2010, **58**, 7376-7382.
16. H. H. Tønnesen, *Die Pharmazie*, 2002, **57**, 820-824.
17. C.-C. Lin, H.-Y. Lin, H.-C. Chen, M.-W. Yu and M.-H. Lee, *Food Chemistry*, 2009, **116**, 923-928.
18. A. Anitha, S. Maya, N. Deepa, K. Chennazhi, S. Nair, H. Tamura and R. Jayakumar, *Carbohydrate Polymers*, 2011, **83**, 452-461.
19. K. Avgoustakis, A. Beletsi, Z. Panagi, P. Klepetsanis, E. Livaniou, G. Evangelatos and D. Ithakissios, *International Journal of Pharmaceutics*, 2003, **259**, 115-127.
20. Y.-A. Shieh, S.-J. Yang, M.-F. Wei and M.-J. Shieh, *ACS nano*, 2010, **4**, 1433-1442.
21. T. Wang and N. He, *Nanoscale*, 2010, **2**, 230-239.
22. X. Wang, L. Yang, Z. G. Chen and D. M. Shin, *CA: a cancer journal for clinicians*, 2008, **58**, 97-110.
23. S. Zhou, X. Deng and H. Yang, *Biomaterials*, 2003, **24**, 3563-3570.
24. M. Gou, X. Wei, K. Men, B. Wang, F. Luo, X. Zhao, Y. Wei and Z. Qian, *Current drug targets*, 2011, **12**, 1131-1150.
25. H. Danafar, S. Davaran, K. Rostamizadeh, H. Valizadeh and M. Hamidi, *Advanced pharmaceutical bulletin*, 2014, **4**, 501.
26. H.-s. Shi, X. Gao, D. Li, Q.-w. Zhang, Y.-s. Wang, Y. Zheng, L.-L. Cai, R.-m. Zhong, A. Rui and Z.-y. Li, *International journal of nanomedicine*, 2012, **7**, 2601.
27. A. Safavy, K. P. Raisch, S. Mantena, L. L. Sanford, S. W. Sham, N. R. Krishna and J. A. Bonner, *Journal of medicinal chemistry*, 2007, **50**, 6284-6288.
28. G. Guo, S. Fu, L. Zhou, H. Liang, M. Fan, F. Luo, Z. Qian and Y. Wei, *Nanoscale*, 2011, **3**, 3825-3832.
29. K. Men, M. L. Gou, Q. F. Guo, X. H. Wang, S. Shi, B. Kan, M. J. Huang, F. Luo, L. J. Chen and X. Zhao, *Journal of nanoscience and nanotechnology*, 2010, **10**, 7958-7964.
30. H. Danafar, K. Rostamizadeh, S. Davaran and M. Hamidi, *Drug development and industrial pharmacy*, 2014, **40**, 1411-1420.
31. Z. Song, R. Feng, M. Sun, C. Guo, Y. Gao, L. Li and G. Zhai, *Journal of colloid and interface science*, 2011, **354**, 116-123.
32. S. Bisht, G. Feldmann, S. Soni, R. Ravi, C. Karikar, A. Maitra and A. Maitra, *J Nanobiotechnology*, 2007, **5**, 1-18.
33. A. Anitha, V. Deepagan, V. D. Rani, D. Menon, S. Nair and R. Jayakumar, *Carbohydrate Polymers*, 2011, **84**, 1158-1164.
34. S. Rajabi, A. Ramazani, M. Hamidi and T. Naji, *DARU Journal of Pharmaceutical Sciences*, 2015, **23**, 20.

35. J. m. Xu, S. t. Song, Z. m. Tang, Z. f. Jiang, X. q. Liu, L. Zhou, J. Zhang and X. w. Liu, *Breast cancer research and treatment*, 1999, **53**, 77-85.
36. S. L. Fink and B. T. Cookson, *Infection and immunity*, 2005, **73**, 1907-1916.
37. C. Vestergaard, H. Yoneyama, M. Murai, K. Nakamura, K. Tamaki, Y. Terashima, T. Imai, O. Yoshie, T. Irimura and H. Mizutani, *Journal of Clinical Investigation*, 1999, **104**, 1097.
38. N. T. Huynh, M. Morille, J. Bejaud, P. Legras, A. Vessieres, G. Jaouen, J.-P. Benoit and C. Passirani, *Pharmaceutical research*, 2011, **28**, 3189-3198.
39. E. S. Vitetta, S. Baur and J. W. Uhr, *The Journal of experimental medicine*, 1971, **134**, 242-264.
40. S. X. Leng, J. E. McElhaney, J. D. Walston, D. Xie, N. S. Fedarko and G. A. Kuchel, *The Journals of Gerontology Series A: Biological Sciences and Medical Sciences*, 2008, **63**, 879-884.
41. B. Xu, J. Yuan, T. Ding and Q. Gao, *Polymer bulletin*, 2010, **64**, 537-551.
42. C. B. Liu, C. Y. Gong, M. J. Huang, J. W. Wang, Y. F. Pan, Y. D. Zhang, G. Z. Li, M. L. Gou, K. Wang and M. J. Tu, *Journal of Biomedical Materials Research Part B: Applied Biomaterials*, 2008, **84**, 165-175.
43. L. Piao, Z. Dai, M. Deng, X. Chen and X. Jing, *Polymer*, 2003, **44**, 2025-2031.
44. H. S. Choi, W. Liu, P. Misra, E. Tanaka, J. P. Zimmer, B. I. Ipe, M. G. Bawendi and J. V. Frangioni, *Nature biotechnology*, 2007, **25**, 1165-1170.
45. C. Mohanty and S. K. Sahoo, *Biomaterials*, 2010, **31**, 6597-6611.
46. R. Joshi, Vanderbilt University, 2011.
47. I. Chattopadhyay, K. Biswas, U. Bandyopadhyay and R. K. Banerjee, *Current science*, 2004, **87**, 44-53.
48. R. K. Maheshwari, A. K. Singh, J. Gaddipati and R. C. Srimal, *Life sciences*, 2006, **78**, 2081-2087.
49. A. Goel and B. B. Aggarwal, *Nutrition and cancer*, 2010, **62**, 919-930.
50. A. Kumari, S. K. Yadav and S. C. Yadav, *Colloids and Surfaces B: Biointerfaces*, 2010, **75**, 1-18.
51. K. Xiao, Y. Li, J. Luo, J. S. Lee, W. Xiao, A. M. Gonik, R. G. Agarwal and K. S. Lam, *Biomaterials*, 2011, **32**, 3435-3446.
52. P. Aggarwal, J. B. Hall, C. B. McLeland, M. A. Dobrovolskaia and S. E. McNeil, *Advanced drug delivery reviews*, 2009, **61**, 428-437.
53. G. P. Mishra, University of Missouri--Kansas City, 2011.

Figures caption

Figure 1.H NMR spectrum of PCL-PEG-PCL tri-block copolymer in CDCl3.

Figure 2.GPC spectrum of PCL-PEG-PCL copolymer.

Figure 3. AFM image of micelles

Figure 4. Particle size distribution and zeta potential of CUR/PCL-PEG-PCL micelles (a) particle size distribution (b) zeta potential

Figure 5. FT-IR spectra of (a) curcumin, (b) PCL-PEG-PCL and, (c) CUR - PCL-PEG-PCL micelles .

Figure 6. DSC spectra of (a) PCL-PEG-PCL, (b) curcumin and (c)CUR - PCL-PEG-PCL micelles.

Figure 7. The release profiles of curcumin from CUR- PCL-PEG-PCL micelles in different release media (a) PH= 7.4, (b) plasma, (c) pH=5.5, (d) free curcumin release pH=7.4.

Figure 8. Cytotoxicity effects of CUR@ [PCL-PEG-PCL] NPs on (A) MCF-7, (B) PC3, (C) 4T1 as cancerous cells; and (D) MCF10a as normal cell were measured.

Figure 9. The apoptosis induction by CUR@ [PCL-PEG-PCL] NPs on (a) MCF-7, and (b) 4T1cell line.

Figure 10.The expression in MCF-7 cell lines treated void CUR, PCL-PEG-PCL micelles and CUR@ [PCL-PEG-PCL] NPs. The gene expression profile of c-myc, bax, bcl-xl, and bcl-2 were analyzed with GAPDH that used as internal control. Each bar represents the mean ± S.D. $P < 0.05$, statistically significantly compared with untreated control.

Figure 11. Changes in tumor volume and survival rate of mice after treatment. A, CUR,PCL-PEG-PCL nanoformulation significantly inhibits tumor growth as of day 21 following injection of cancerous cells compared to mice receiving void curcumin as well as control groups; [PCL-PEG-PCL] NPs and PBS. The values are mean ±SD of tumor volumes (n=6 mice per group). B, Survival curve of different groups illustrates that mice receiving CUR, PCL-PEG-PCL nanoformulation survived longer than those in the other groups. Representative data for one of two experiments has been shown.

Figure 12. Body weight changes in 4T1 tumor cell xenograft mice. Values are expressed as Mean ± SD of six mice (g). All animals at sacrifice and Day 0 (initiation day of treatment) were overnight fasted; curcumin loaded nanoparticle and void curcumin were intraperitoneally administered at 12.5 mg/kg BW (body weight).

Figure13. Proliferation indexes of splenocytes from mice in the presence of tumor lysate, PHA and medium. A, Data achieved by MTT assay shows a significant difference in lymphocyte production between mice receiving Cur@pcl-PEG-pcl and three other groups treated with void curcumin, pcl-PEG-pcl and PBS. B and C, without any significant difference in splenocytes proliferation amongst groups. The mean of ±SD of triplicate determinations are indicated (n=6 mice per group). *Significantly different to mice receiving Cur@pcl-PEG-pcl and PBS (n=6 mice per group).

Figure14. a) IFN-γ and b) IL-4 are produced by splenocytes in mice receiving cur@ PCL-PEG-PCL. There is a significant difference in IFN-γ and IL-4 production in mice treated with cur@ pcl-peg -pcl compared to three other groups given void curcumin, pcl-peg -pcl and PBS. The mean ±SD of triplicate determinations are shown (n=4mice per group). Representative data from one of two experiments have been shown. *Significantly different from other groups. **Significantly different from pcl-peg -pcl and PBS groups.

Table 1.Molecular characterics of the synthesized copolymer

Copolymer	CL / EG feed	M_n(KDa) [a]	M_w (KDa)[a]	PdI[b]	T_m (°C) [c]	DP_{PEG}	DP^d_{PCL}
PCL-PEG-PCL	0.5	17.5	20.4	1.16	58.68	136.36	126.16

a: Determined by GPC analysis using narrow molecular weight polystyrene standards.

b: M_w/M_n = Polydispersity index of the polymers (PdI) determined by GPC analysis

c: Calculated from the first run of DSC as half of the extrapolated tangents

d: DP: degree of polymerization

Table 2. Stability of nanoparticles suspension

micelles	Mean size of micelles immediately after preparation (nm)	Mean size of micelles after 15 day (nm)	Mean size of micelles after 30 days (nm)
CUR- PCL-PEG-PCL micelles	99.07	125	150.2

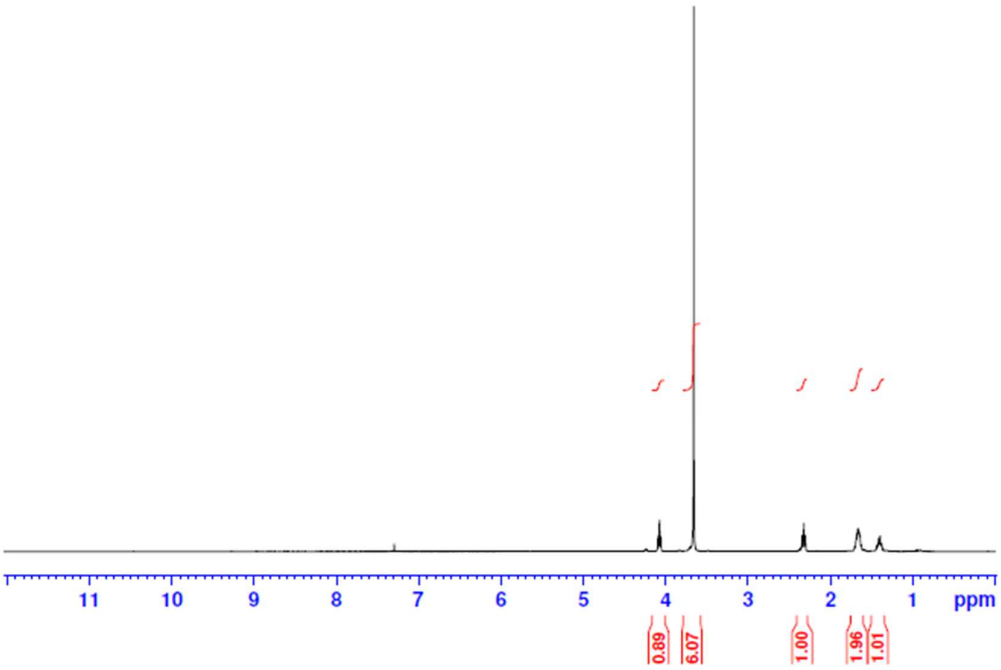

Figure 1.

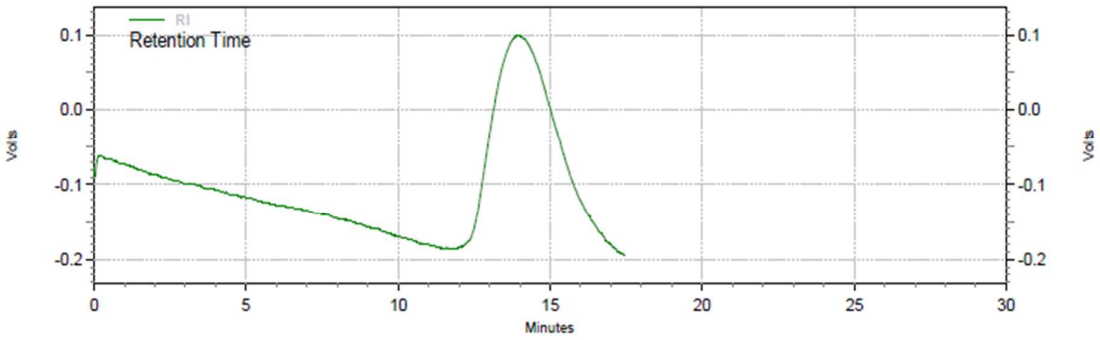

Figure 2.

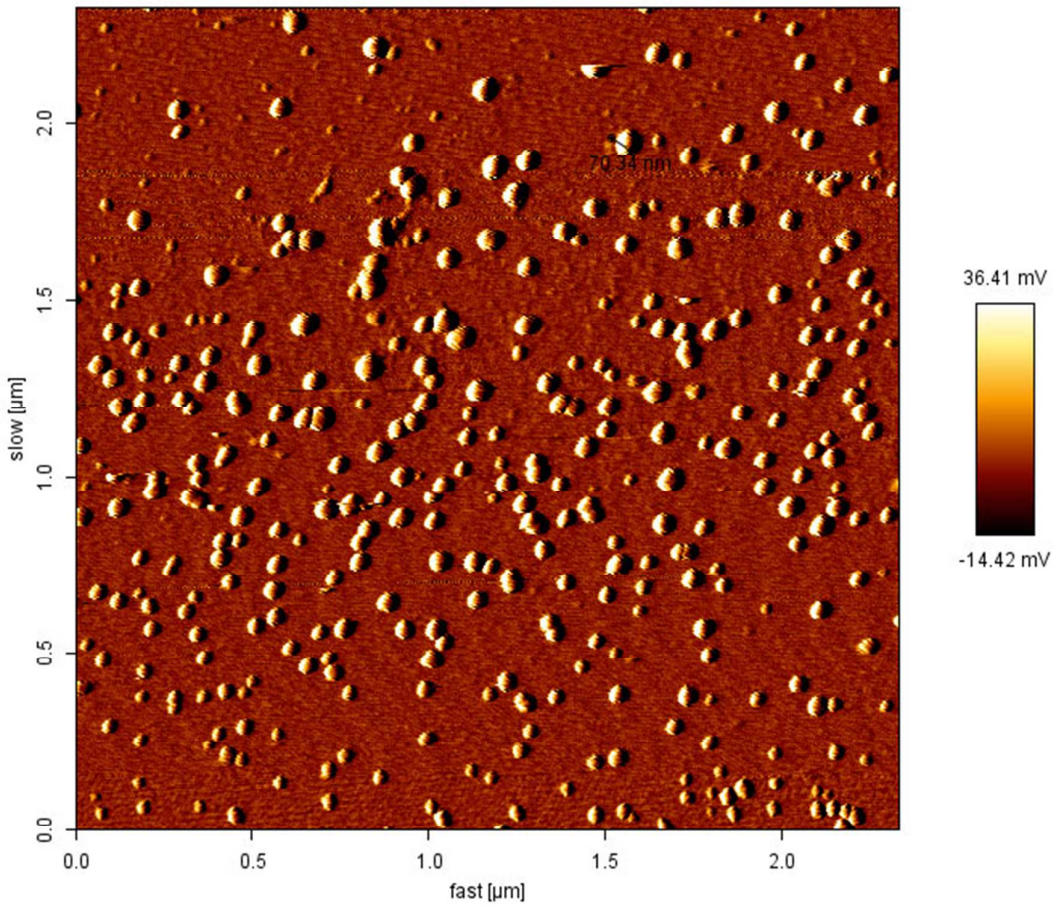

Figure 3.

a)

		Size (d.nm):	% Intensity	Width (d.n...
Z-Average (d.nm): 99.07	Peak 1:	115.7	98.9	51.63
PdI: 0.181	Peak 2:	4818	1.1	715.7
Intercept: 0.898	Peak 3:	0.000	0.0	0.000
Result quality : Good				

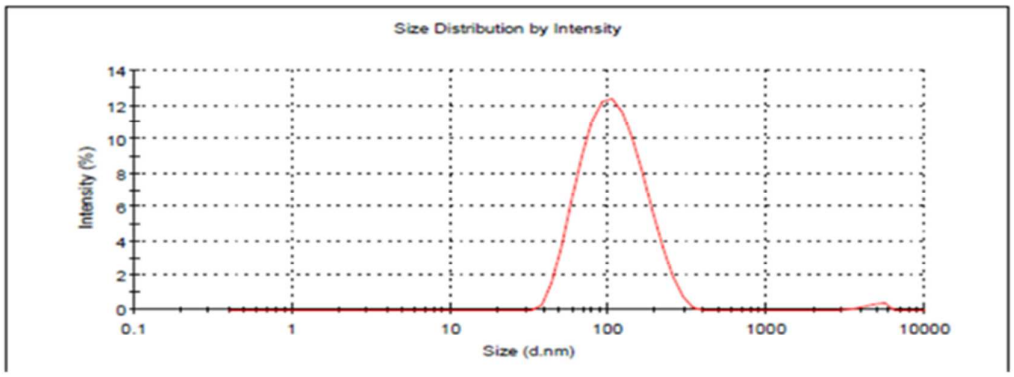

b)

		Mean (mV)	Area (%)	Width (mV)
Zeta Potential (mV): -5.58	Peak 1:	-5.58	100.0	4.47
Zeta Deviation (mV): 4.47	Peak 2:	0.00	0.0	0.00
Conductivity (mS/cm): 0.0822	Peak 3:	0.00	0.0	0.00
Result quality : Good				

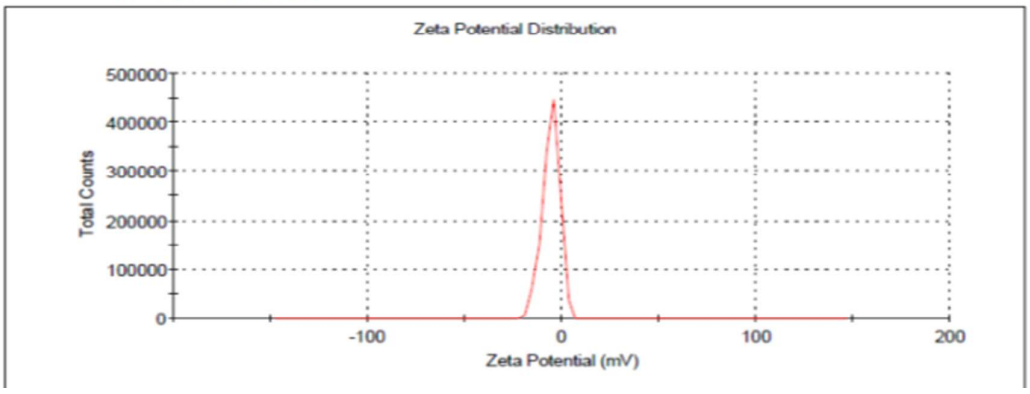

Figure 4.

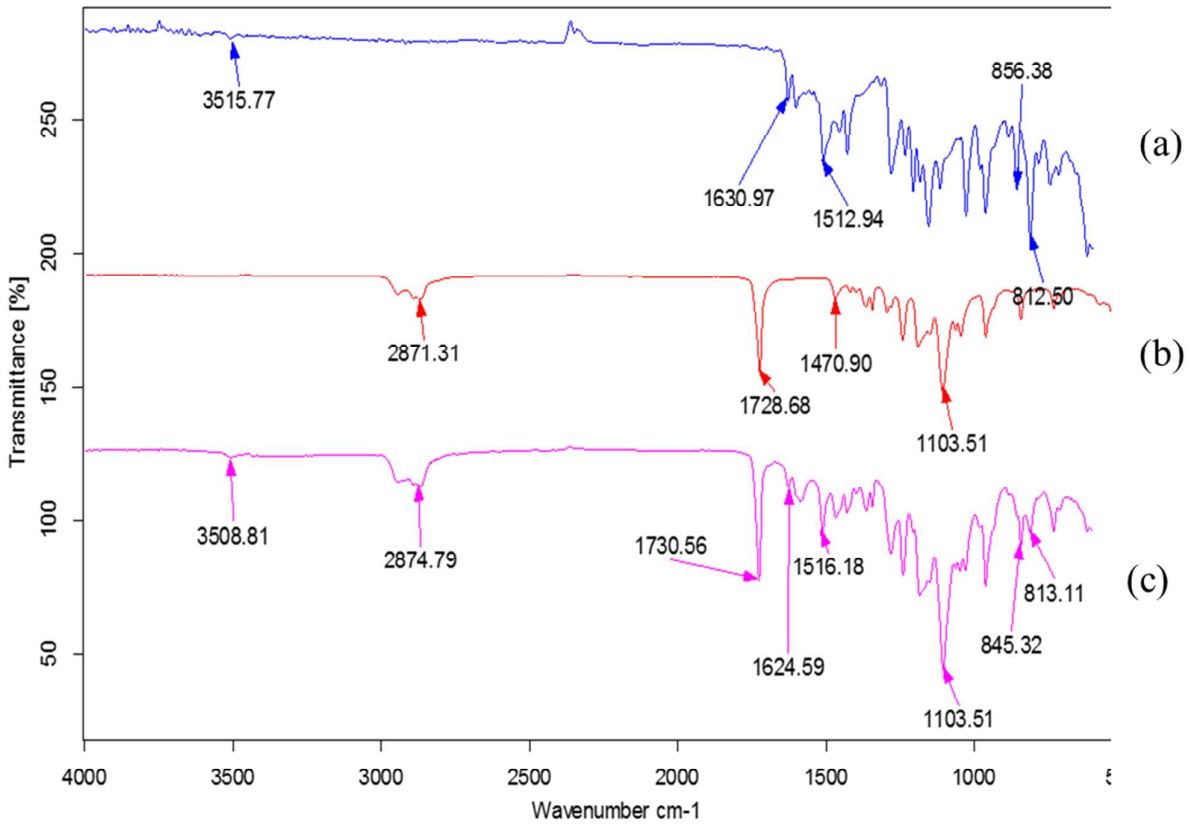
Transmittance [%]
250
200
150
100
50
3515.77
1630.97
1512.94
856.38
812.50
(a)
2871.31
1728.68
1470.90
1103.51
(b)
3508.81
2874.79
1730.56
1624.59
1516.18
1103.51
845.32
813.11
(c)
4000
3500
3000
2500
2000
1500
1000
Wavenumber cm-1

Figure 5.

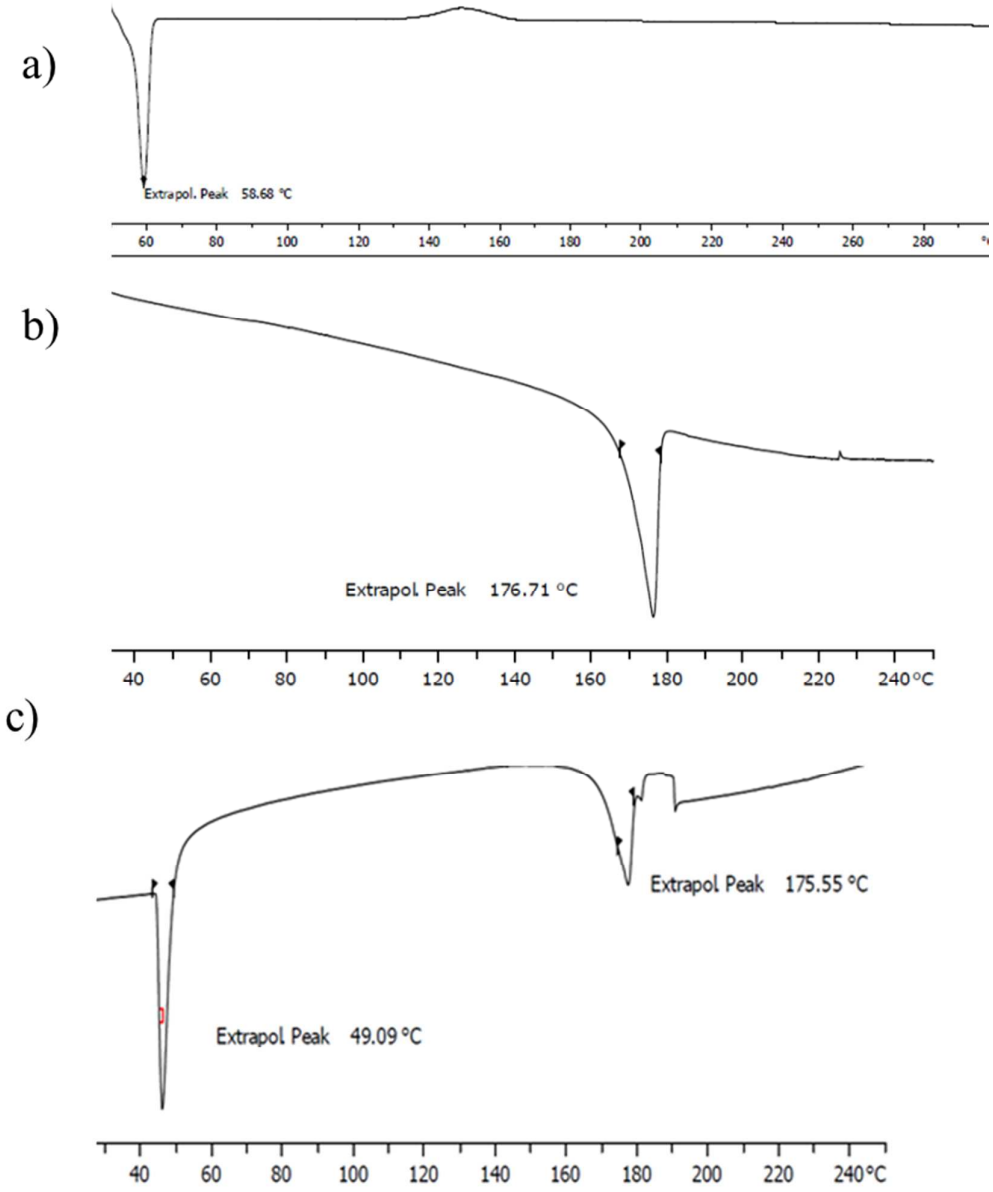
a)
Extrapol. Peak 58.68 °C
60 80 100 120 140 160 180 200 220 240 260 280
b)
Extrapol Peak 176.71 °C
40 60 80 100 120 140 160 180 200 220 240 °C
c)
Extrapol Peak 175.55 °C
Extrapol Peak 49.09 °C
40 60 80 100 120 140 160 180 200 220 240 °C

Figure 6.

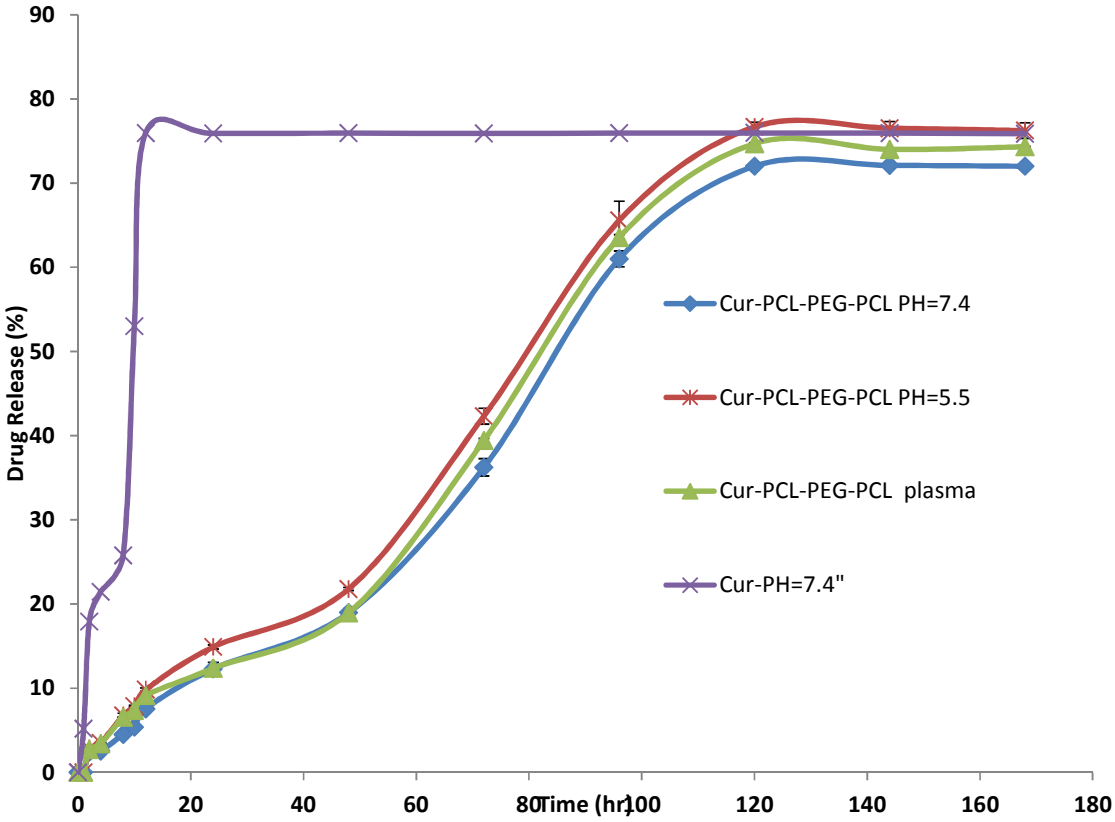
90
80
70
60
50
40
30
20
10
0
Drug Release (%)
0
20
40
60
80
100
120
140
160
180
Time (hr)
Cur-PCL-PEG-PCL PH=7.4
Cur-PCL-PEG-PCL PH=5.5
Cur-PCL-PEG-PCL plasma
Cur-PH=7.4"

Figure 7.

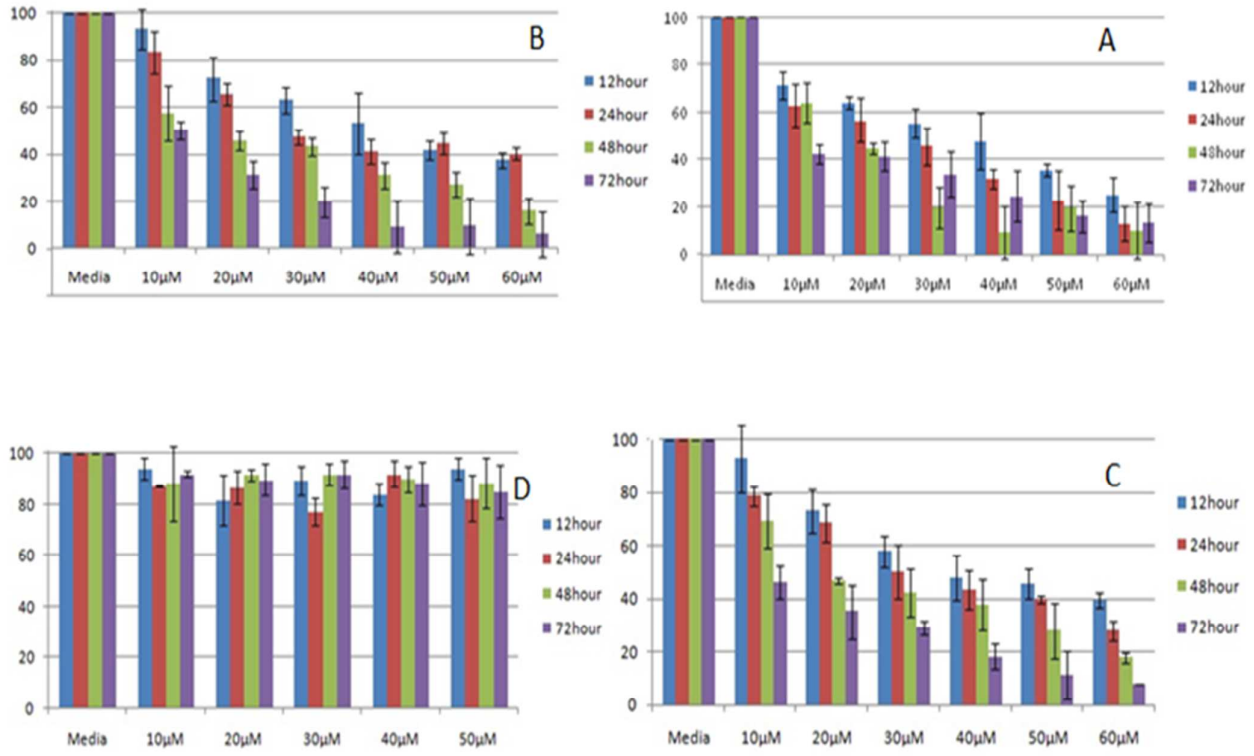

Figure 8.

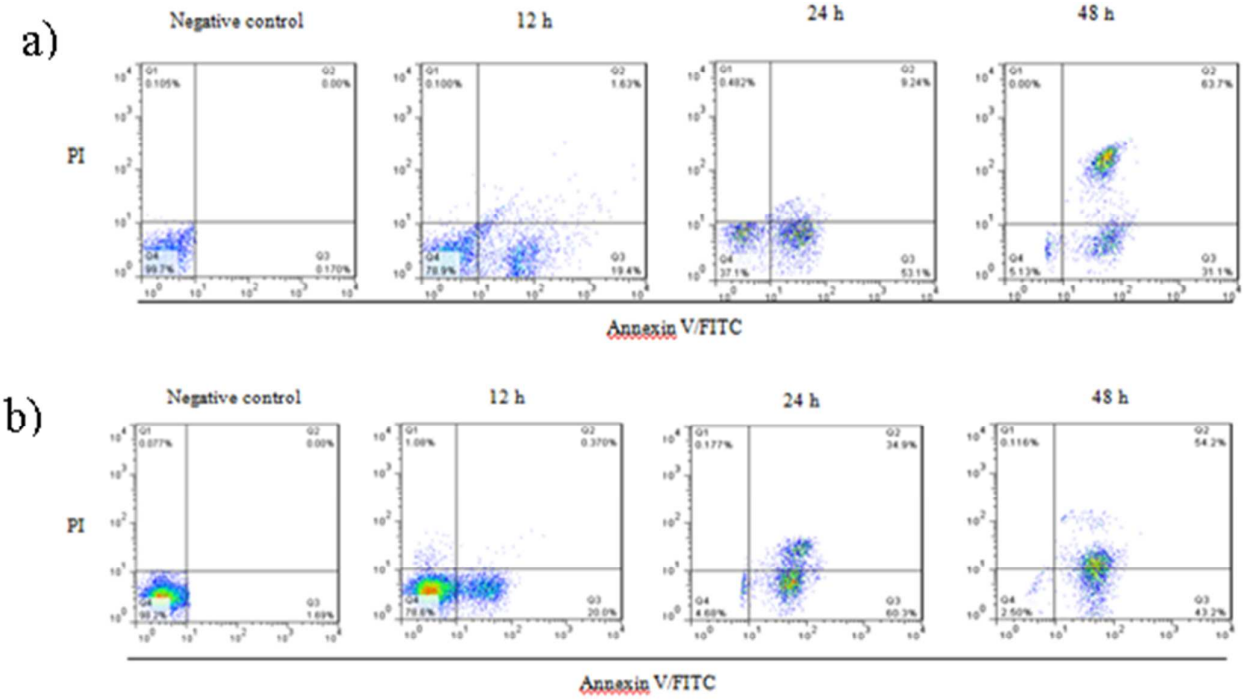

Figure 9.

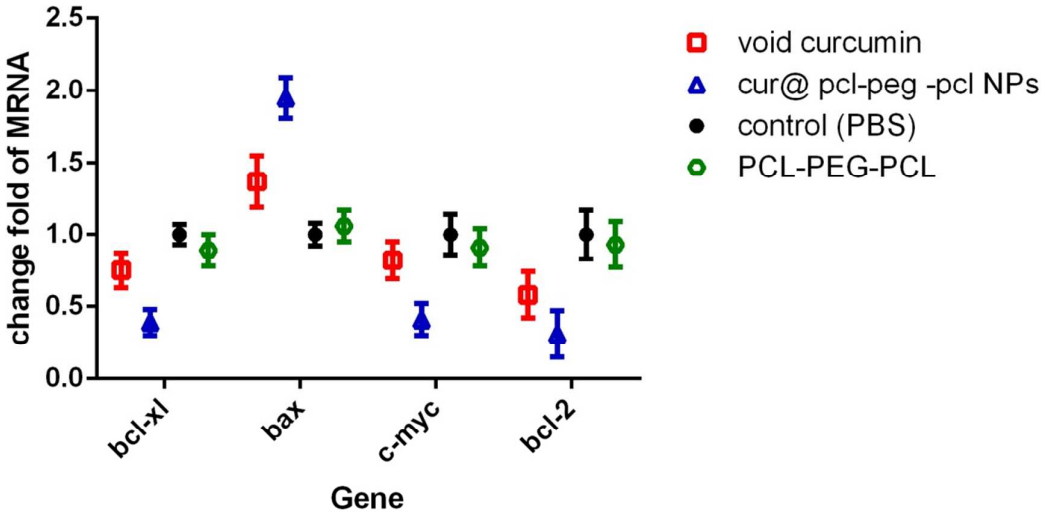

Figure 10

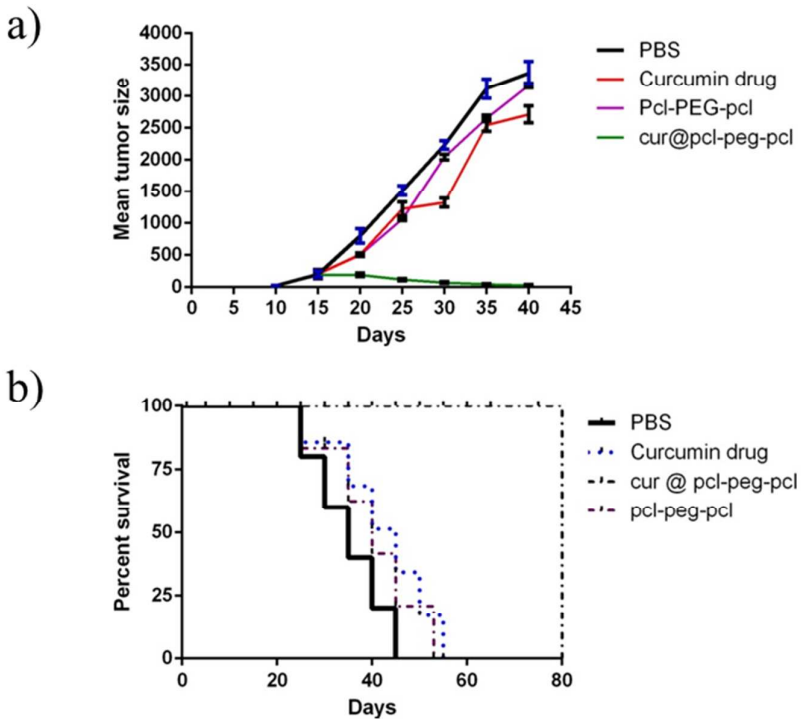

Figure 11

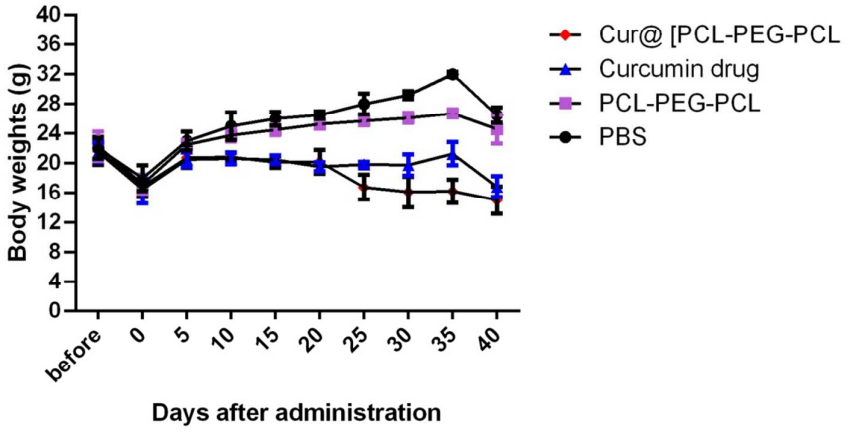
Body weights (g)
40
36
32
28
24
20
16
12
8
4
0
before
0
5
10
15
20
25
30
35
40
Days after administration
Cur@ [PCL-PEG-PCL
Curcumin drug
PCL-PEG-PCL
PBS

Figure. 12

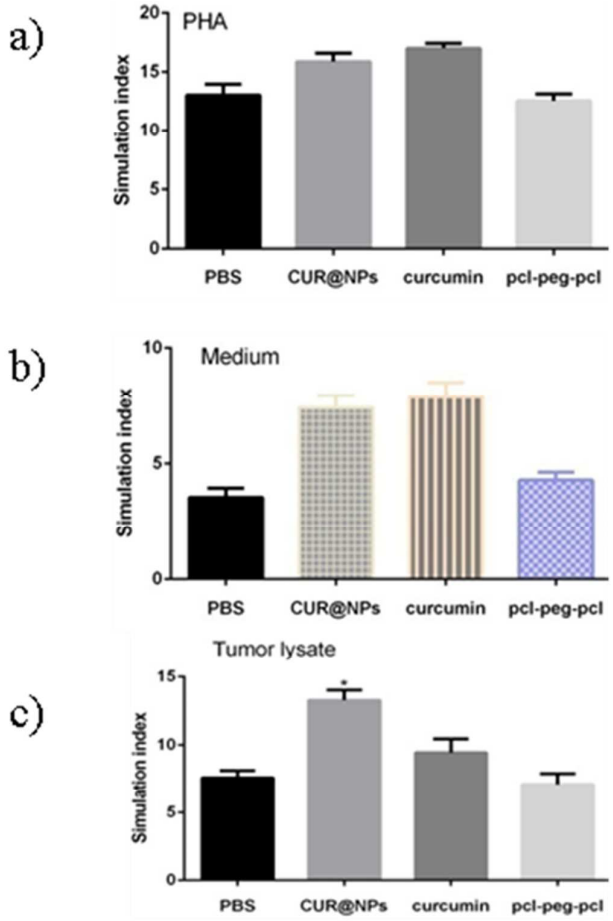
a)
PHA
Simulation index
20
15
10
5
0
PBS
CUR@NPs
curcumin
pcl-peg-pcl
b)
Medium
Simulation index
10
5
0
PBS
CUR@NPs
curcumin
pcl-peg-pcl
c)
Tumor lysate
Simulation index
15
10
5
0
PBS
CUR@NPs
curcumin
pcl-peg-pcl

Figure 13

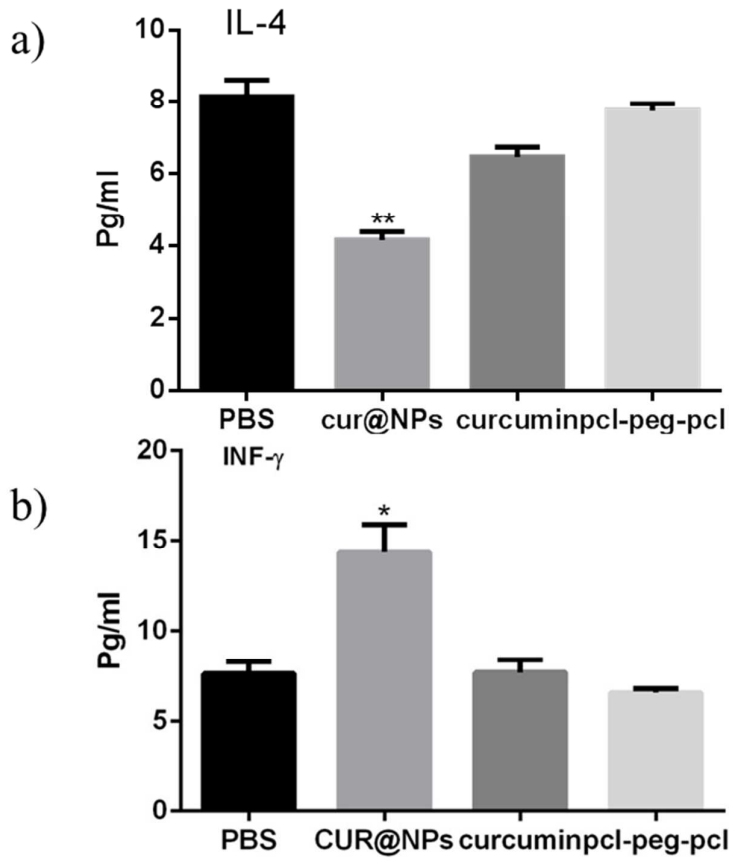
a)
IL-4
Pg/ml
10
8
6
4
2
0
**
PBS
cur@NPs
curcuminpcl-peg-pcl
b)
INF-γ
Pg/ml
20
15
10
5
0
*
PBS
CUR@NPs
curcuminpcl-peg-pcl

Figure 14

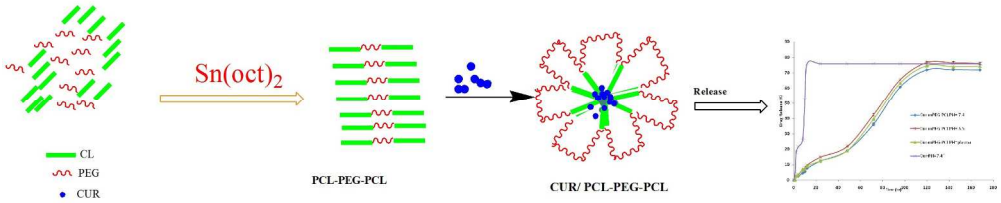

211x43mm (300 x 300 DPI)